NeuroImage: Clinical 13 (2017) 55–61

Contents lists available at ScienceDirect

NeuroImage: Clinical

journal homepage: www.elsevier.com/locate/ynicl

Altered structural and functional thalamocortical networks in secondarily generalized extratemporal lobe seizures

Syu-Jyun Peng[a], Yue-Loong Hsin[b,*]

[a] Biomedical Electronics Translational Research Center, National Chiao Tung University, 1001 University Rd., Hsinchu City 300, Taiwan
[b] Department of Neurology, Chung Shan Medical University and Chung Shan Medical University Hospital, No. 110, Sec. 1, Jianguo N. Rd., South Dist., Taichung City 40201, Taiwan

ARTICLE INFO

Article history:
Received 7 July 2016
Received in revised form 7 November 2016
Accepted 11 November 2016
Available online 12 November 2016

Keywords:
Thalamocortical network
Generalized seizure
Gray matter density
Fractional anisotropy

ABSTRACT

Structural and functional abnormalities in the thalamocortical network in primary generalized epilepsies or mesial temporal lobe epilepsy have recently been identified by voxel-wise analyses of neuroimaging. However, evidence is needed regarding the profiles of the thalamocortical network in patients with secondarily generalized seizures from focal neocortical sources. We used high-resolution T1-weighted, diffusion-tensor and resting-state functional MR imaging (rs-fMRI) to examine 16 patients with secondarily generalized extratemporal lobe seizures and 16 healthy controls. All the patients were medically effective and MRI-negative. Using whole brain voxel-based morphometry (VBM) to compare the patients with the normal controls, we observed significantly decreased gray matter (GM) density in the thalamus and 3 frontal gyri and significantly reduced white matter (WM) fractional anisotropy (FA) in the bilateral anterior corona radiata of the patients. Alterations in the thalamocortical functional connectivity with different cortices were identified by the rs-fMRI analysis seeding of the whole thalamus. The prefrontal gyri with the greatest functional connectivity were also traced by seeding a sub-thalamic region that is demarcated in an atlas, in which the thalamic parcellation is based on the WM connectivity to the cortices. This sub-thalamic region anatomically contains the mediodorsal thalamic nucleus where, concordantly, there was a significant decrease in thalamic GM density in the VBM study. In contrast to the negative correlation between the disease duration and reduced thalamic densities and subcortical FA values, the strength of the functional thalamocortical connectivity had a paradoxical correlation. Our results conclusively indicate that generalized seizures with a focal cortical source are associated with structural and functional alterations in the thalamocortical network.

1. Introduction

In both primary and secondarily generalized seizures, the electroclinical features, such as bilateral stiffening, jerking of limbs, or bilateral synchronous EEG discharge, suggest that there is a system responsible for the dynamic connection between the bilateral hemispheres during the phase.

The thalamus, one of the deep brain structures, is reciprocally linked with the cerebral cortex. Widespread cortical connections are assumed to be involved in the bilateral synchronization or propagation of epileptic electricity. In addition to previous electrophysiological studies implicating the thalamus in epileptogenesis, emerging technologies used in the acquisition and processing of neuroimaging have allowed the further characterization of the structural and functional connections between the cerebral cortex and the thalamus.

With respect to the structures of the thalamocortical network, volume changes in the thalami and alterations of nerve tract imaged parameters have been found in patients with idiopathic generalized epilepsies (IGEs) and mesial temporal lobe epilepsy (mTLE) through group comparisons using voxel-wise statistics (Keller and Roberts, 2008; Focke et al., 2014; Ciumas and Savic, 2006). Extending the voxel-wise comparison to address the functions of the thalamocortical network, functional alterations in the thalamocortical network were found in patients with IGEs and mTLE (Kim et al., 2014; Keller et al., 2014; Chen et al., 2015).

However, the methods used to investigate the structural and functional connectivity of the thalamocortical network have rarely been employed in patients with secondarily generalized seizures from focal cortical sources. In this study, we investigated the structural and functional connectivity of the thalamocortical network in a medically effective patient group identified as having a history of generalized convulsions, a localizable seizure source beyond the medial temporal region and no visible lesions on magnetic resonance imaging (MRI). We studied the structural difference by measuring the gray matter (GM) density via T1-weighted MRI, the white matter (WM) integrity

* Corresponding author.
E-mail addresses: blue.year@msa.hinet.net (S.-J. Peng), hsin.yloong@msa.hinet.net (Y.-L. Hsin).

http://dx.doi.org/10.1016/j.nicl.2016.11.010

via diffusion tensor imaging (DTI), and the functional connectivity via resting-state functional MRI (rs-fMRI). Our aim was to identify changes in the structures of the thalamus and thalamus associated fiber bundles and the functional connection between the thalamus and cortex. In the event of any change in the thalamocortical network, we further examined the possible progression of that change.

2. Methods and materials

2.1. Subjects

We retrospectively reviewed the clinical database of Hualien Tzu Chi General Hospital to collect MR data of patients with secondarily generalized seizures. We excluded patients as "lesional" when the radiologists identified any questionable lesions on the MRIs (such as possible sclerotic or atrophic changes in the mesial temporal lobe or possible blurred gray-white matter junction). Patients who possibly had mTLE with maximal interictal or ictal epileptiform discharges localized to the temporal lobe and with classic semiological features of mTLE were excluded. Patients who probably had conventionally termed primarily generalized epilepsies with symmetric interictal or ictal epileptiform discharges and non-lateralized presentations of clinical seizures were also excluded. Recruited patients were categorized as having pharmacoresponsive epilepsy, with a rare seizure recurrence (less than once every 6 months) under mono antiepileptic therapy. We further collected MRI data from age-matched healthy subjects as a control group. The study protocol, which consisted of retrospectively analyzing the patients' images and collecting images from the control subjects, was approved by the ethics committee of Buddhist Tzu Chi General Hospital in Hualien, Taiwan, and written informed consent was obtained from each control participant.

2.2. Image acquisition

At the Tzu Chi Hospital, most patients with epilepsy are studied with an epilepsy-specific protocol that includes an acquisition session for rs-fMRI and standard structure imaging sessions. In this study, the control subjects were imaged with the same imaging sequences. MRI was performed on a SIGNA HDX 1.5T (GE, Milwaukee, WI, USA) with an eight-channel phased-array head coil. A high-resolution axial 3D T1-weighted structure image was acquired using a fast-spoiled gradient-recalled echo (SPGR) sequence with the following parameters: repetition time (TR) = 14.024 ms; echo time (TE) = 14.024 ms; flip angle = 15°; field of view (FOV) = 220 × 220 mm^2; matrix = 256 × 256; and slice thickness = 1 mm. The DTIs were acquired axially using a single-shot spin-echo echo-planar sequence with the following parameters: TR = 8000 ms; TE = 82.4 ms; flip angle = 15°; FOV = 250 × 250 mm^2; matrix = 256 × 256; slice thickness = 3 mm; number of excitations, 2; 25 gradient directions with a b value of 1000 s/mm^2; and 1 null tensor image with a b value of 0 s/mm^2. The rs-fMRI data were obtained using an echo-planar imaging sequence with the following parameters: TR = 2.223 ms; TE = 35 ms; flip angle = 90°; field of view = 240 × 240 mm^2; matrix = 64 × 64; and slice thickness = 4 mm. During the functional scans, the subjects were instructed to keep their eyes closed, not to think about anything and stay awake during the entire session. After the scanning, the subjects were asked whether they remained awake during the entire procedure.

2.3. Statistical analyses of the structural MRIs

Voxel-based morphometry (VBM) analyses were performed using VBM8 (http://dbm.neuro.uni-jena.de/vbm/) a toolbox of SPM8 (http://www.fil.ion.ucl.ac.uk/spm/) running on MATLAB R2014a (The MathWorks, Natick, MA, USA) to compare the density of the GM and the integrity of the WM between the patients and controls. Each individual SPGR image was registered into the null tensor image space and then reoriented with the original set close to the anterior commissure. The registered SPGR images were then segmented into GM, WM, and cerebrospinal fluid probability maps using a segment procedure of the SPM8 module (Ashburner and Friston, 2005). We computed the fractional anisotropy (FA) map using the FMRIB Software Library 4.0 package (http://www.fmrib.ox.ac.uk/fsl) (Koay et al., 2006) after the diffusion-weighted data were preprocessed by head motion, eddy current correction and diffusion tensor fitting. Referring to a standard Montreal Neurological Institute (MNI) template, GM probability and FA maps were transformed non-linearly and readjusted to the voxel size of 3 × 3 × 3 mm^3 using the high-dimensional DARTEL algorithm (Ashburner, 2007). To account for local compression and expansion caused by linear and non-linear transformations, we modulated the images using Jacobian determinants of the deformations (Good et al., 2001). Finally, the modulated GM probability and FA maps were smoothed using a 4 mm FWHM isotropic Gaussian kernel. To identify the differences in the GM density and the WM isotropy between patients and controls, we performed a *t*-test comparison between the two groups, and a double statistical threshold was used (combined height threshold $p < 0.05$ and a minimum cluster size = 16 voxels, as determined by the AlphaSim correction by REST software from http://www.restfmri.net/forum/REST V1.7) (Song et al., 2011). The regions with significantly different GM densities and FA values were further correlated with disease duration by a linear regression analysis. Differences with a p value <0.05 were considered significant.

In addition to VBM, Tract-Based Spatial Statistics (TBSS) functionality of FSL was also used to perform voxel-wise statistical analysis of the FA data. First, the mean diffusion metrics (FA) in the WM skeleton were extracted for each subject. Then, TBSS of the FA images was carried out using TBSS in the FMRIB software library (FSL 4.1.9; www.fmrib.ox.ac.uk/fsl) (Smith et al., 2006).

2.4. Statistical analyses of the functional MRIs

The first 10 scans of rs-fMRI data were removed to allow for magnetization equilibrium. The slice-timing correction was based on the middle slice. The functional data were realigned to the first dynamic scan by rigid body correction, and six parameters of the head movements were then generated. Participants who exhibited head motion >1 mm of translation or 1° of rotation were excluded. The data were then normalized to the MNI space with voxel size resampling of 3 × 3 × 3 using the DARTEL toolbox. Subsequently, a 4-mm FWHM Gaussian kernel was applied for smoothing. The images were then band-pass filtered within 0.01 to 0.08 Hz following a linear detrend to reduce the effects of high-frequency noise and low-frequency drift. To remove spurious signals that were unlikely to reflect neural activity, several nuisance covariates were eliminated by the linear regression. These covariates included the six head motion parameters, the global mean signal, the WM signal, and the cerebrospinal fluid signal.

One entire thalamic seed and seven thalamic subregion seeds were generated in the MNI template utilizing the AAL map (http://www.mccauslandcenter.sc.edu/mricro/) and Oxford thalamic connectivity atlas (Tzourio-Mazoyer et al., 2002; Behrens et al., 2003), respectively. The mean time series for the entire thalamus and each of the seven thalamic subregions was calculated by averaging the time series of all voxels within each seed. The correlation maps were obtained by conducting Pearson's correlation analyses on the time series of each seed and voxel across the whole brain. The resulting correlation coefficients for each voxel (r values) were converted to z scores using Fisher's r-to-z transformation to improve the normality of their distribution. The statistical analyses of the z-scaled functional connectivity data were conducted using REST software. Two-tailed two-sample *t*-tests ($p < 0.05$) were performed for the second-level analysis to determine the significance of the differences in the z-scaled functional connectivity values for the entire thalamus and each of the seven thalamic subregions. An AlphaSim correction was applied after each *t*-test to correct

Table 1
The demographic and clinical data.

Case	Gender	Age	Disease duration	Seizure semiology	EEG	Pharmacotherapy
1	M	22	3	CPS	Rt F	CBZ
2	F	41	19	CPS	Lt F	VPA
3	F	26	6	CPS	Rt F	TPM
4	F	35	16	CPS	Bil. F/T	PHT
5	F	41	16	CPS	Lt F	LVT
6	M	21	4	CPS	Rt O	OXC
7	F	23	6	CPS	Rt F	LMT
8	F	46	27	CPS	Lt F/T	OXC
9	F	33	12	SP	Rt F/T	LMT
10	F	57	35	CPS	Lt F	VPA
11	M	30	6	CPS	Rt F	VPA
12	F	44	26	CPS	Rt F	LMT
13	F	26	8	CPS	Lt F	LMT
14	M	22	3	SP	Rt P	OXC
15	M	27	15	CPS	Lt F/T	OXC
16	M	29	9	SP	Lt P	OXC

Lt = left, Rt = right, Bil. = bilateral;
F = frontal, T = temporal, P = parietal, O = occipital;
CPS = complex partial seizure, SP = simple partial seizure;
CBZ = carbamazepine, LMT = lamotrigine, OXC = oxicarbazepine, PHT = phenytoin, TPM = topiramate, VPA = valproic acid, LVT = levetiracetam.

for the multiple comparisons. Those clusters with significantly altered z-scaled functional connectivity values were further correlated with the disease duration. Statistical significance was considered at $p < 0.05$.

3. Results

Ultimately, MRI data from 16 patients [6 males and 10 females, mean age = 32.7 ± 10.5 years (mean ± standard deviation)] fitting our inclusion criteria were collected. One patient had occipital lobe epilepsy and exhibited elementary visual hallucination at seizure onset. Two patients had parietal lobe epilepsy with paresthetic sensation at onset. Six patients had seizure focus over the left frontotemporal regions and exhibited cessation of talking at onset or postictal aphasia. Seven patients had maximal seizure EEG activity over the right or bilateral frontopolar regions at onset (Table 1). Sixteen healthy controls without a history of neurological or psychiatric symptoms that were similar in age and gender [6 males and 10 females, mean age = 33.1 ± 10.1 years] to the seizure patient group were also recruited.

3.1. Differences in structural connectivity

Compared to the controls, patients exhibited significant regional GM density reductions in the thalamus ($p < 0.01$, cluster size = 33 voxels, peak t-score = −4.03, MNI coordinate = 0/−12/6), left postcentral gyrus ($p < 0.01$, cluster size = 26 voxels, peak t-score = −4.39, MNI coordinate = −27/−42/54), left superior frontal gyrus ($p < 0.01$, cluster size = 18 voxels, peak t-score = −3.46, MNI coordinate = −18/15/54), and left supplementary motor area ($p < 0.01$, cluster size = 92 voxels, peak t-score = −4.28, MNI coordinate = −9/0/78) (Fig. 1). At the same threshold, no area of increased GM density was found in patients compared to the controls.

Through a VBM analysis, the patients exhibited significantly decreased FA values in the left external capsule ($p < 0.01$, cluster size = 28 voxels, peak t-score = −3.65, MNI coordinate = −30/12/−3), left anterior corona radiata ($p < 0.01$, cluster size = 26, peak t-score = −3.47, MNI coordinate = −21/24/15) and right anterior corona radiata ($p < 0.01$, one cluster size = 33 voxels, peak t-score = −4.54, MNI coordinate = 24/24/15; another cluster size = 19 voxels, peak t-score = −3.60, MNI coordinate = 21/15/21) (Fig. 2). No increase in FA value was detected in the patients. TBSS did not reveal any difference on the diffusion map skeletons of FA between the patients and controls.

3.2. Differences in functional connectivity

The seed-to-whole-brain connectivity analysis stemming the whole thalamus showed significantly increased connection with the cortices of the left inferior temporal gyrus, right inferior frontal gyrus, left middle frontal gyrus, and right superior frontal gyrus in the patient group. Decreased values of functional connectivity were found in the right insula and right midcingulate area (Table 2 and Fig. 3A).

Many cortical areas showed significantly different functional connections with the 7 sub-thalamic regions individually when the seed-to-whole-brain analysis based on each sub-thalamic seed was segmented according to the WM connectivity to the gyri (Table 3). In the sub-thalamic region 4 that is responsible for the prefrontal cortical area, functional connectivity highly increased in the right inferior frontal and right superior frontal gyri were spatially accordant with the results of the whole thalamic seed analysis (Fig. 3B).

3.3. Correlations with disease duration

The GM density of the thalamus was significantly and negatively correlated with the duration of disease ($R = 0.730$, $p = 0.001$). Negative correlations between FA values and the duration of epilepsy were observed in the left external capsule ($R = 0.620$, $p = 0.010$; not showed in Fig. 4) and the bilateral anterior corona radiata ($R = 0.701$, $p = 0.003$). The strength of connection with the left middle frontal gyrus was positively correlated with disease duration ($R = 0.515$, $p = 0.041$). The strength of connection with the left inferior temporal gyrus was negatively correlated with disease duration ($R = 0.504$, $p = 0.047$; not showed on Fig. 4). The left middle frontal gyrus showed a positive correlation with disease duration and was significantly and negatively correlated with the FA of bilateral anterior corona radiata ($R = 0.520$, $p = 0.039$) (Fig. 4).

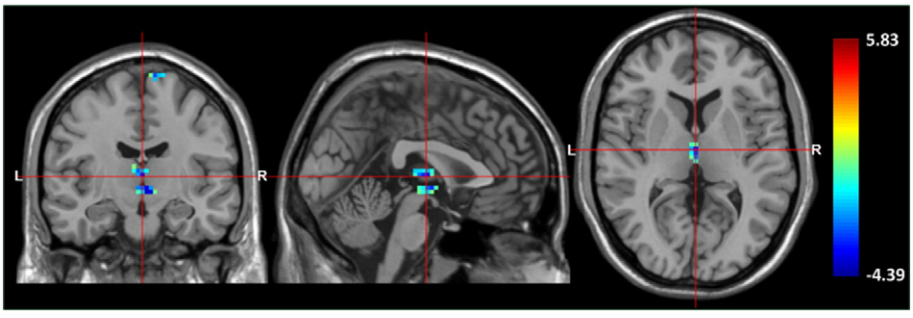

Fig. 1. Statistical parametric maps superimposed on standard T1 MRI template images show a significant GM density reduction in the bilateral thalami in patients compared to control (AlphaSim correction, $p < 0.01$, minimum cluster size threshold of 16 voxels). The color bar represents the t-score.

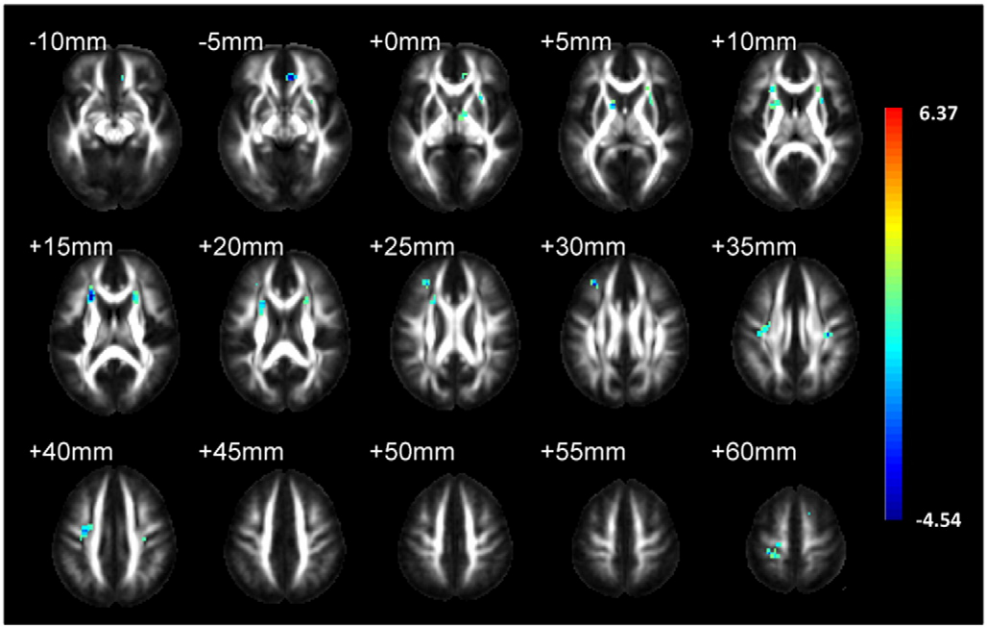

Fig. 2. Statistic parametric maps superimposed on the international consortium of brain mapping template for FA map show the clusters of significant FA value reduction (AlphaSim correction, $p < 0.01$, minimum cluster size threshold of 16 voxels). The color bar shows the *t*-score and the magnitude of the significant difference.

4. Discussion

Early neurophysiological studies investigating the relationship between the thalamus and cortex suggested the role of the thalamus in primary and secondarily generalized epilepsies (Dempsey and Morison, 1941; Jasper and Droogleever-Fortuyn, 1947). Numerous research studies have continued to attempt to correlate the thalamus and the related cortico-subcortical network with epilepsies, especially with recent improvements in neuroimaging techniques. The voxel-wise comparison is the most commonly used method to investigate the differences in brain structures or functional connectivity between experimental and control groups (Ashburner and Friston, 2000). To conduct group-averaged statistical comparisons across the whole brain, normalization algorithms must align each participant's anatomy to a template image able to account for differences. Therefore, it is rational that most studies in patients with mTLE or IGEs address this issue for the similar locations of the seizure focus, the pathologic changes and even the genetic etiologies. In this study, we investigated the structural and functional connectivity between the thalamus and neocortex of patients with secondary general convulsions originating outside of the mesial temporal region. To compensate for the irrationality to group patients with different locations of seizure focus, we excluded patients with lesional MRI. Most patients in the present study had seizures from the frontal lobe, but all of them had secondarily generalized convulsions. The possibility of cortical dysplasia should also be considered in patients with "non-lesional MRI" (Hauptman and Mathern, 2012; Lerner et al., 2009). Investigation of the thalamocortical networks of this patient group is needed as MRI-negative pharmacoresistant focal epilepsy patients are the most challenging for conventional epilepsy surgery but are possibly responsive to modern neuromodulation therapy, i.e., thalamic stimulation. Although our patients were pharmacoeffetive and had rare seizure generalizations, their thalamic GM density, WM integrity, and functional thalamocortical connectivity were still different from those of the healthy subjects.

Previous VBM studies focusing on thalamic differences have reported volume atrophy of the thalamus in patients with IGEs and mTLE. Diverse atrophied regions within the thalamus have been reported across many studies in patients with IGEs, including mediodorsal atrophy in childhood absence epilepsy (Chan et al., 2006; Pardoe et al., 2008), and ventromedial, mediodorsal or anteriomedial atrophies in other generalized epilepsies (Helms et al., 2006; Wang et al., 2012; Kim et al., 2013). In patients with mTLE, previous studies were most consistent with one another regarding findings of atrophy in the mediodorsal nucleus of the thalamus (Barron et al., 2012; Bernhardt et al., 2012; Keller et al., 2014), which is in agreement with our observation that the peak MNI coordinate location of the reduced thalamus cluster density was over the mediodorsal region. Centeno et al. did not find thalamic volume changes in patients with frontal lobe epilepsy using VBM analysis. The fact that 11 of the 43 patients they investigated had identifiable cortical dysplasia and the possibility that not all the patients had secondary generalization might have confounded their results (Centeno et al., 2014).

In the monkey, the mediodorsal nucleus is reciprocally connected to the prefrontal cortex (Tobias, 1975). In Behrens's early human study, a large mediodorsal region of the thalamus had highly probable prefrontal and temporal connections (Behrens et al., 2003). DTI allows for the detection of microstructural alterations in WM. The FA value is one of the commonly used parameters for grading WM integrity. Previous DTI studies identified abnormalities in the integrity of WM in both children (Nilsson et al., 2008) and adults with epilepsies (Duncan, 2008; Yogarajah and Duncan, 2008). Our WM FA measurements indicated low FA values in the bilateral anterior corona radiata and left external capsule away from the main frames of their fiber tracts. The anterior corona radiata contains fibers running from the thalamus to the frontal

Table 2
Regions of significant thalamic functional connectivity differences.

Regions	MNI coordinate	Peak *t*-score	Number of voxels
L inferior temporal gyrus*	−45, −12, −27	3.4418	62
R insula*	36, 6, 12	−4.2155	76
R inferior frontal gyrus**	33, 18, 21	4.43	28
L middle frontal gyrus*	−36, 6, 36	3.0978	68
R midcingulate area*	6, −39, 39	−3.3348	82
R superior frontal gyrus**	18, 48, 48	4.62	43

SPM maps were thresholded at $^{**}p < 0.01$ and $^{*}p < 0.05$ (AlphaSim correction, voxel-level, minimum cluster size threshold of 16 voxels).
R: right; MNI: Montreal Neurological Institute.

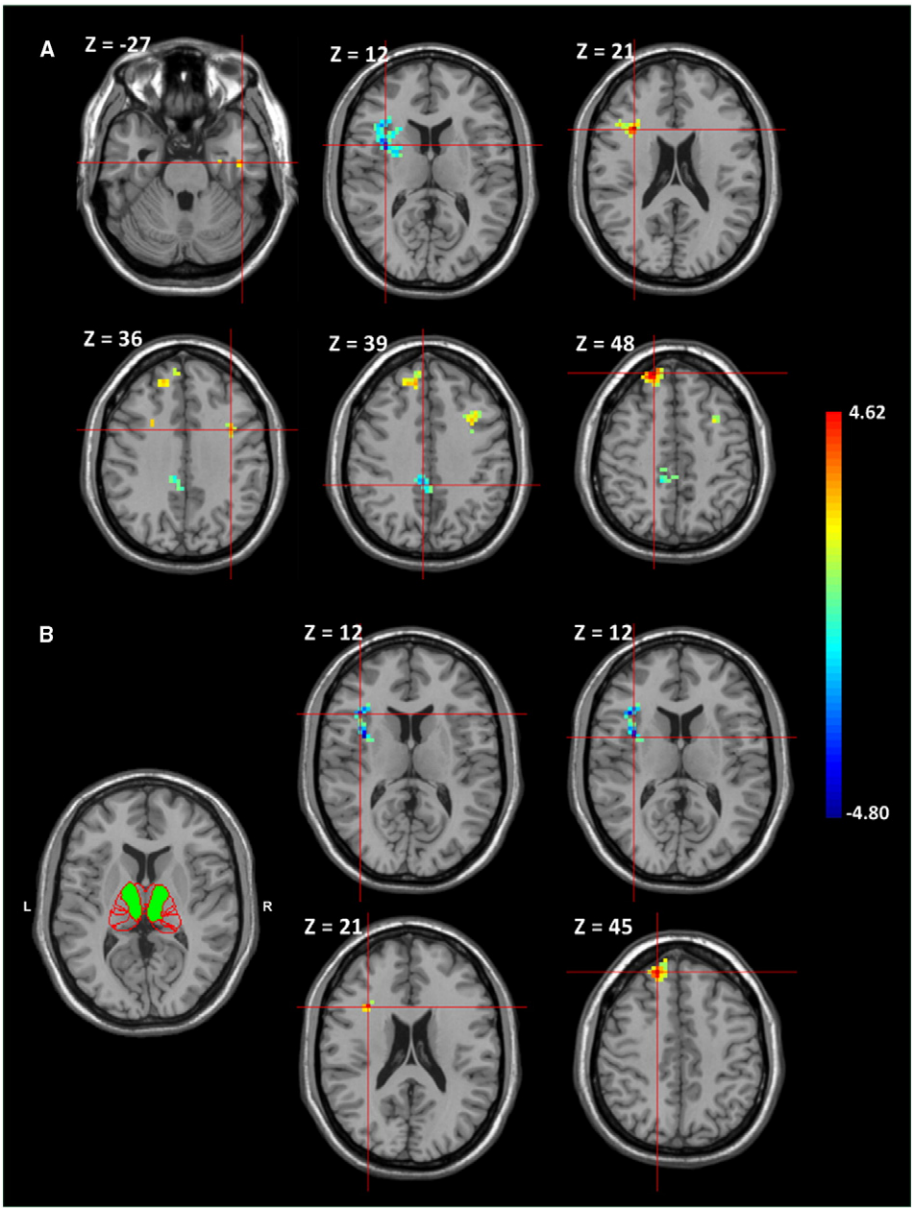

Fig. 3. Between-group comparisons of thalamocortical FC. A Significant increases of thalamocortical FC in the left inferior temporal gyrus, right inferior frontal gyrus, left middle frontal gyrus, and right superior frontal gyrus and decreases in the right insula and right midcingulate area are shown in patients compared to controls. B The thalamus parcellation atlas composed of a green sub-region 4, which is responsible for the prefrontal cortical area. Significantly increased FC between sub-thalamic region 4 and the right inferior frontal gyrus and right superior frontal gyrus and decreases in the right inferior frontal gyrus and right insula are shown in patients compared to controls. The color bar represents the *t*-score.

Table 3
Thalamic subregions of significant functional connectivity differences.

Thalamic subregion	Significant regions	
1	Increased	R middle frontal gyrus; L postcentral gyrus; R superior frontal gyrus; L sub-gyral; L precentral gyrus
	Decreased	Lobule IV, V of vermis; L middle frontal gyrus; R extra-nuclear; L insula
2	Increased	L lingual Gyrus
	Decreased	Lobule III of vermis; R caudate nucleus
3	Increased	L extra-nuclear; L supplementary motor area
	Decreased	R hippocampus; R superior temporal pole; R precuneus; R caudate nucleus; L superior parietal lobule
4	Increased	R inferior frontal gyrus; R superior frontal gyrus
	Decreased	R inferior frontal gyrus; R insula
5	Increased	R gyrus rectus; R superior frontal gyrus; R middle frontal gyrus
	Decreased	Lobule III of vermis; L middle frontal gyrus; R putamen; R midcingulate area
6	Increased	L inferior frontal gyrus; L precentral gyrus; L supplementary motor area
	Decreased	R lobule VIII of cerebellar hemisphere; R caudate nucleus; L insula
7	Increased	R precentral gyrus
	Decreased	R midcingulate area

Thalamic subregions 1 responsible for primary motor cortical region, 2 responsible for sensory cortical region, 3 responsible for occipital cortical region, 4 responsible for prefrontal cortical region, 5 responsible for premotor cortical region, 6 responsible for posterior parietal cortical region, 7 responsible for temporal cortical region; R: right; L: left.

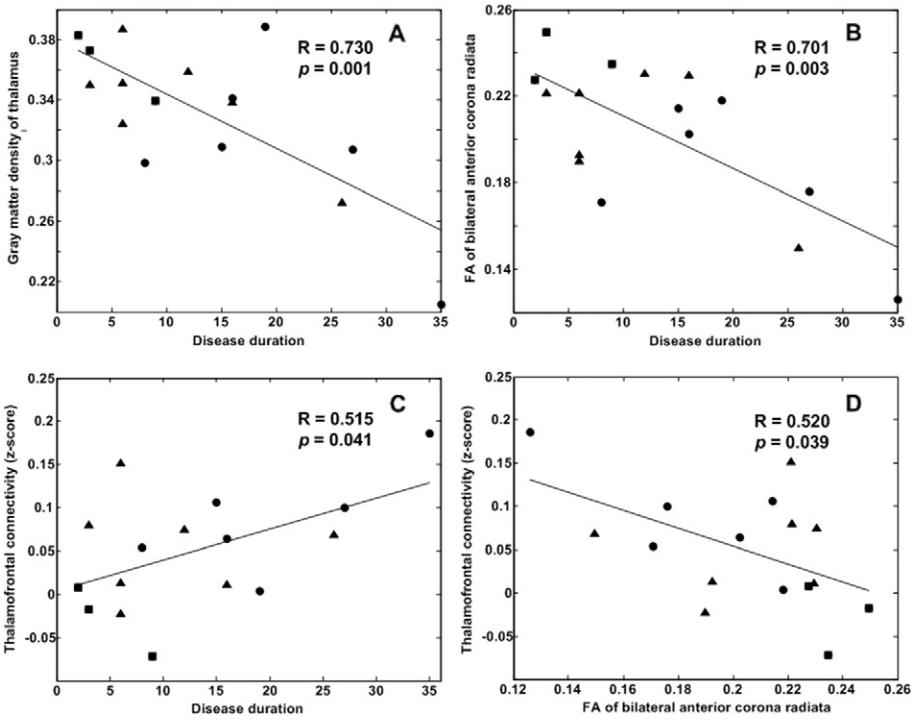

Fig. 4. Relationship between GM density, FA values, functional connectivity strength and the duration of epilepsy. A The GM density of the thalamus was negatively correlated with the disease duration. B The FA values of the bilateral anterior corona radiata were negatively correlated with the disease duration. C The disease duration was positively correlated with the functional connectivity strength of the left middle frontal gyrus. D The functional connectivity strength of the left middle frontal gyrus was negatively correlated with the FA values of the bilateral anterior corona radiata. The circles represent patients with left frontotemporal seizures. The triangles represent patients with right/bilateral frontopolar seizures. The squares represent the others.

lobe. Briefly, the anatomic connections between the mediodorsal nucleus and prefrontal cortex in this patient group are still different.

In addition to alterations in the associated structures in the thalamocortical connections, rs-fMRI studies have provided further evidence indicating that aberrant networks are related to seizure generalization. Using a VBM comparison of 49 patients with IGEs, Kim et al. demonstrated a reduction in thalamocortical functional connectivity in the bilateral medial prefrontal cortex and posterior cingulated cortex through functional connectivity analysis seeding at the anteriomedial thalamus (Kim et al., 2014). Another fMRI study using thalamic seeding found decreased functional connectivity between the thalamic mediodorsal nucleus and the bilateral orbital frontal cortex (Wang et al., 2012). He et al. provided evidence of decreased regional specific thalamocortical functional connectivity in patients with TLE. They also demonstrated that the bilateral thalamocortical functional connectivity decreases in patients with secondary generalization (He et al., 2015). In contrast to our fMRI analysis, some cortices demonstrated high functional connections with the thalamus in this patient group. Two frontal gyri exhibited intense functional connectivity with the whole thalamus and were spatially correlated to sub-thalamic region 4. According to the Oxford thalamic connectivity atlas, the sub-thalamic region 4 has been shown to involve a part of the mediodorsal thalamic nucleus.

The reduction of thalamic volume and WM linearity further correlated with the disease duration in our patients with a very low seizure frequency. These findings are consistent with the results obtained by many previous studies in which researchers identified changes in WM integrity in patients with IGEs and mTLE and correlated those changes with clinical variables, including disease duration (Liu et al., 2011; Deppe et al., 2008; Arfanakis et al., 2002; Gross, 2011; Lee et al., 2004; Riley et al., 2010). Labate et al. observed GM decreases in the thalami of patients with hippocampal sclerosis and normal MRI with mild TLE (Labate et al., 2008; Labate et al., 2010). In a longitudinal MRI follow-up study of seizure-free TLE patients, Alvim and her colleagues not only found diffuse extrahippocampal GM atrophy but also clarified the progression of the GM atrophy (Alvim et al., 2016). Kim et al. found a negative correlation between the disease duration and the thalamocortical FC strength of the bilateral medial prefrontal cortex in patients with IGEs (Kim et al., 2014). Similar to our findings of the paradoxical alteration of the functional and structural thalamocortical connections, strengthened functional connectivity may play a critical role in seizure generalization.

Because the location of these groupings is quite different, it is rational to expect that the networks involved in epileptogenesis, seizure initiation, and spread are different. One larger group (the 7 patients with right or bilateral frontopolar seizures) possibly drove the results. However, the relationship between disease duration and GM density change, FA alteration, and thalamocortical connectivity in the different subgroups remained.

5. Conclusion

In summary, our results indicate that generalized seizures with focal cortical sources are associated with structural and functional alterations of the thalamocortical network even when there are no visible brain lesions. Although our findings do not directly indicate existing alterations of the thalamocortical network in patients at seizure onset, there is still possible progression in the deformation of the thalamocortical networks.

Conflicts of interest

None of the authors have any conflict of interest.

Acknowledgments

This work was supported in part by the Ministry of Science and Technology, Taiwan, under the project MOST 105-2218-E-009-027 and in part by the “Aim for the Top University Plan” of National Chiao Tung University and the Ministry of Education, Taiwan.

References

Alvim, M.K., Coan, A.C., Campos, B.M., Yasuda, C.L., Oliveira, M.C., Morita, M.E., Cendes, F., 2016. Progression of gray matter atrophy in seizure-free patients with temporal lobe epilepsy. Epilepsia 57, 621–629.

Arfanakis, K., Hermann, B.P., Rogers, B.P., Carew, J.D., Seidenberg, M., Meyerand, M.E., 2002. Diffusion tensor MRI in temporal lobe epilepsy. Magn. Reson. Imaging 20, 511–519.

Ashburner, J., 2007. A fast diffeomorphic image registration algorithm. NeuroImage 38, 95–113.

Ashburner, J., Friston, K.J., 2000. Voxel-based morphometry–the methods. NeuroImage 11, 805–821.

Ashburner, J., Friston, K.J., 2005. Unified segmentation. NeuroImage 26, 839–851.

Barron, D.S., Fox, P.M., Laird, A.R., Robinson, J.L., Fox, P.T., 2012. Thalamic medial dorsal nucleus atrophy in medial temporal lobe epilepsy: a VBM meta-analysis. Neurol. Clin. 2, 25–32.

Behrens, T.E., Johansen-Berg, H., Woolrich, M.W., Smith, S.M., Wheeler-Kingshott, C.A., Boulby, P.A., Barker, G.J., Sillery, E.L., Sheehan, K., Ciccarelli, O., Thompson, A.J., Brady, J.M., Matthews, P.M., 2003. Non-invasive mapping of connections between human thalamus and cortex using diffusion imaging. Nat. Neurosci. 6, 750–757.

Bernhardt, B.C., Bernasconi, N., Kim, H., Bernasconi, A., 2012. Mapping thalamocortical network pathology in temporal lobe epilepsy. Neurology 78, 129–136.

Centeno, M., Vollmar, C., Stretton, J., Symms, M.R., Thompson, P.J., Richardson, M.P., O'Muircheartaigh, J., Duncan, J.S., Koepp, M.J., 2014. Structural changes in the temporal lobe and piriform cortex in frontal lobe epilepsy. Epilepsy Res. 108, 978–981.

Chan, C.H., Briellmann, R.S., Pell, G.S., Scheffer, I.E., Abbott, D.F., Jackson, G.D., 2006. Thalamic atrophy in childhood absence epilepsy. Epilepsia 47, 399–405.

Chen, X.M., Huang, D.H., Chen, Z.R., Ye, W., Lv, Z.X., Zheng, J.O., 2015. Temporal lobe epilepsy: decreased thalamic resting-state functional connectivity and their relationships with alertness performance. Epilepsy Behav. 44, 47–54.

Ciumas, C., Savic, I., 2006. Structural changes in patients with primary generalized tonic and clonic seizures. Neurology 67, 683–686.

Dempsey, E.W., Morison, R.S., 1941. The production of rhythmically recurrent cortical potentials after localized thalamic stimulation. Am. J. Physiol. 135, 293–300.

Deppe, M., Kellinghaus, C., Duning, T., Moddel, G., Mohammadi, S., Deppe, K., Schiffbauer, H., Kugel, H., Keller, S.S., Ringelstein, E.B., Knecht, S., 2008. Nerve fiber impairment of anterior thalamocortical circuitry in juvenile myoclonic epilepsy. Neurology 71, 1981–1985.

Duncan, J.S., 2008. Imaging the brain's highways-diffusion tensor imaging in epilepsy. Epilepsy Curr. 8, 85–89.

Focke, N.K., Diederich, C., Helms, G., Nitsche, M.A., Lerche, H., Paulus, W., 2014. Idiopathic-generalized epilepsy shows profound white matter diffusion-tensor imaging alterations. Hum. Brain Mapp. 35, 3332–3342.

Good, C.D., Johnsrude, I.S., Ashburner, J., Henson, R.N., Friston, K.J., Frackowiak, R.S., 2001. A voxel-based morphometric study of ageing in 465 normal adult human brains. NeuroImage 14, 21–36.

Gross, D.W., 2011. Diffusion tensor imaging in temporal lobe epilepsy. Epilepsia 52 (Suppl. 4), 32–34.

Hauptman, J.S., Mathern, G.W., 2012. Surgical treatment of epilepsy associated with cortical dysplasia: 2012 update. Epilepsia 53 (Suppl. 4), 98–104.

He, X., Doucet, G.E., Sperling, M., Sharan, A., Tracy, J.I., 2015. Reduced thalamocortical functional connectivity in temporal lobe epilepsy. Epilepsia 56, 1571–1579.

Helms, G., Ciumas, C., Kyaga, S., Savic, I., 2006. Increased thalamus levels of glutamate and glutamine (glx) in patients with idiopathic generalised epilepsy. J. Neurol. Neurosurg. Psychiatry 77, 489–494.

Jasper, H.H., Droogleever-Fortuyn, J., 1947. Experimental studies of the functional anatomy of petit ma1 epilepsy. Res. Publ. Assoc. Res. Nerv. Ment. Dis. 26, 272–298.

Keller, S.S., Roberts, N., 2008. Voxel-based morphometry of temporal lobe epilepsy: an introduction and review of the literature. Epilepsia 49, 741–757.

Keller, S.S., O'Muircheartaigh, J., Traynor, C., Towgood, K., Barker, G.J., Richardson, M.P., 2014. Thalamotemporal impairment in temporal lobe epilepsy: a combined MRI analysis of structure, integrity, and connectivity. Epilepsia 55, 306–315.

Kim, J.H., Kim, J.B., Seo, W.K., Suh, S.I., Koh, S.B., 2013. Volumetric and shape analysis of thalamus in idiopathic generalized epilepsy. J. Neurol. 260, 1846–1854.

Kim, J.B., Suh, S.I., Seo, W.K., Oh, K., Koh, S.B., Kim, J.H., 2014. Altered thalamocortical functional connectivity in idiopathic generalized epilepsy. Epilepsia 55, 592–600.

Koay, C.G., Chang, L.C., Carew, J.D., Pierpaoli, C., Basser, P.J., 2006. A unifying theoretical and algorithmic framework for least squares methods of estimation in diffusion tensor imaging. J. Magn. Reson. 182, 115–125.

Labate, A., Cerasa, A., Gambardella, A., Aguglia, U., Quattrone, A., 2008. Hippocampal and thalamic atrophy in mild temporal lobe epilepsy: a VBM study. Neurology 71, 1094–1101.

Labate, A., Cerasa, A., Aguglia, U., Mumoli, L., Quattrone, A., Gambardella, A., 2010. Voxel-based morphometry of sporadic epileptic patients with mesiotemporal sclerosis. Epilepsia 51, 506–510.

Lee, S.K., Kim, D.I., Mori, S., Kim, J., Kim, H.D., Heo, K., Lee, B.I., 2004. Diffusion tensor MRI visualizes decreased subcortical fiber connectivity in focal cortical dysplasia. NeuroImage 22, 1826–1829.

Lerner, J.T., Salamon, N., Hauptman, J.S., Velasco, T.R., Hemb, M., Wu, J.Y., Sankar, R., Donald Shields, W., Engel Jr., J., Fried, I., Cepeda, C., Andre, V.M., Levine, M.S., Miyata, H., Yong, W.H., Vinters, H.V., Mathern, G.W., 2009. Assessment and surgical outcomes for mild type I and severe type II cortical dysplasia: a critical review and the UCLA experience. Epilepsia 50, 1310–1335.

Liu, M., Concha, L., Beaulieu, C., Gross, D.W., 2011. Distinct white matter abnormalities in different idiopathic generalized epilepsy syndromes. Epilepsia 52, 2267–2275.

Nilsson, D., Go, C., Rutka, J.T., Rydenhag, B., Mabbott, D.J., Snead 3rd, O.C., Raybaud, C.R., 2008. and Widjaja E., Bilateral diffusion tensor abnormalities of temporal lobe and cingulate gyrus white matter in children with temporal lobe epilepsy. Epilepsy Res 81, 128–135.

Pardoe, H., Pell, G.S., Abbott, D.F., Berg, A.T., Jackson, G.D., 2008. Multi-site voxel-based morphometry: methods and a feasibility demonstration with childhood absence epilepsy. NeuroImage 42, 611–616.

Riley, J.D., Franklin, D.L., Choi, V., Kim, R.C., Binder, D.K., Cramer, S.C., Lin, J.J., 2010. Altered white matter integrity in temporal lobe epilepsy: association with cognitive and clinical profiles. Epilepsia 51, 536–545.

Smith, S.M., Jenkinson, M., Johansen-Berg, H., Rueckert, D., Nichols, T.E., Mackay, C.E., Watkins, K.E., Ciccarelli, O., Cader, M.Z., Matthews, P.M., Behrens, T.E., 2006. Tract-based spatial statistics: voxelwise analysis of multi-subject diffusion data. NeuroImage 31, 1487–1505.

Song, X.W., Dong, Z.Y., Long, X.Y., Li, S.F., Zuo, X.N., Zhu, C.Z., He, Y., Yan, C.G., Zang, Y.F., 2011. REST: a toolkit for resting-state functional magnetic resonance imaging data processing. PLoS One 6, e25031.

Tobias, T.J., 1975. Afferents to prefrontal cortex from the thalamic mediodorsal nucleus in the rhesus monkey. Brain Res. 83, 191–212.

Tzourio-Mazoyer, N., Landeau, B., Papathanassiou, D., Crivello, F., Etard, O., Delcroix, N., Mazoyer, B., Joliot, M., 2002. Automated anatomical labeling of activations in SPM using a macroscopic anatomical parcellation of the MNI MRI single-subject brain. NeuroImage 15, 273–289.

Wang, Z., Zhang, Z., Jiao, Q., Liao, W., Chen, G., Sun, K., Shen, L., Wang, M., Li, K., Liu, Y., Lu, G., 2012. Impairments of thalamic nuclei in idiopathic generalized epilepsy revealed by a study combining morphological and functional connectivity MRI. PLoS One 7, e39701.

Yogarajah, M., Duncan, J.S., 2008. Diffusion-based magnetic resonance imaging and tractography in epilepsy. Epilepsia 49, 189–200.